Supporting Information

for

Shining light on integrity of a tetracobalt-polyoxometalate water oxidation catalyst by X-ray spectroscopy before and after catalysis

Rafael Schiwon,[b] Katharina Klingan,[a] Holger Dau[a] and Christian Limberg[b]

[a] Freie Universität Berlin, FB Physik, Arnimallee 14, 14195 Berlin,

Germany.

[b] Humboldt-Universität zu Berlin, Institut für Chemie, Brook-Taylor-Str. 2, 12489 Berlin,

Germany,

* To whom correspondence should be addressed:

holger.dau@fu-berlin.de, christian.limberg@chemie.hu-berlin.de

Table of Contents

General procedures. Solvents were purified employing a MBRAUN SOLVENT PURIFICATION SYSTEM SPS. Infrared (IR) spectra were recorded using solid samples prepared as KBr pellets with a SHIMADZU FTIR-8400S-spectrometer. Microanalyses were performed on a LECO CHNS-932 elemental analyser.

Buffer preparation. The solutions were prepared from purified, deionized water (Millipore milliQ water, >18 MΩ·cm). A solution of inorganic sodium phosphate, NaP_i, was prepared as a mixture of ~ 5% NaH_2PO_4 and ~ 95% Na_2HPO_4 at a total P_i concentration of 30 mM. We verified that the pH of the resulting electrolyte was 8.0. Fine adjustment of the pH was achieved by addition of small aliquots of 1 M NaH_2PO_4 or 1 M Na_2HPO_4.

ESI mass spectrometry. Mass spectra (ESI) were recorded on an AGILENT TECHNOLOGIES 6210 Time-of-Flight LC-MS instrument with syringe pump. Spectra were obtained in negative-ion mode, with the capillary held at 5 kV. The drying gas flow rate was 13.0 L/min with a temperature of 230°C. The nebulizer gas was at a pressure of 60 psi / 4 bar. The m/z range detected was from 100 to 2000. The fragmentor was set to 100 V and the skimmer to 50 V. The flow rate of the solution was 600 µL/hour. **1** was dissolved in 80:20 H_2O:MeOH mixture. The sample concentration for **1** was 1 mM and its full mass spectrum is depicted in Figure S2.

UV/Vis spectroscopy. Optical absorption spectra were recorded on an AGILENT 8453 diode array spectrometer in kinetics mode (Figures S9 – S19). The total reaction volume in the cell was 2 mL, which was constantly stirred. The cell was charged with solid $[Ru(bpy)_3](ClO_4)_3$ in a glove box and sealed with a septum; the remaining head space was floated with argon during the measurement. Argon was bubbled for 10 minutes through an aqueous 30 mM NaP_i buffer solution. An aqueous solution of 0.64 mM in **1** in 30 mM NaP_i was obtained through dissolution of 3.5 mg **1** in 1 mL of a 30 mM solution of NaPi which after bubbling argon gas through the solution for exactly 10 minutes was immediately injected to the cell. The decomposition reaction of $[Ru(bpy)_3](ClO_4)_3$ was started with addition of 2 mL of the 30 mM NaP_i buffer solution to 2.6 mg solid $[Ru(bpy)_3](ClO_4)_3$ with a syringe and spectra were recorded every 3 seconds (Figure S9 and S10). Within 20 seconds 10 µL of a solution of 0.64 mM in **1** in 30 mM NaP_i buffer were added, which accelerated decrease of the absorption band of $[Ru(bpy)_3]^{3+}$ at λ = 670 nm immediately (Figure S11 and S12). The final reaction concentrations were 3.2 µM in **1** and 1.5 mM in $[Ru(bpy)_3](ClO_4)_3$.

Under air 1 mL of a 2 mM aqueous solution of **1** was mixed with 1 mL of H_2O (Figure S13 and S14) or 1 mL of a 60 mM solution in NaP_i (30 mM in NaPi, Figure S15 and S16) or 1 mL of a 800 mM solution in NaP_i (400 mM in NaP_i, Figure S17 and S18) to get a 1 mM solution in **1** and spectra were recorded every 10 seconds for 90 minutes in a quartz cuvette (1 cm path length). Spectra were corrected by subtracting the average extinction between 700-800 nm. All three time traces (Figure S14, S16, S18) (H_2O, 30 mM and 400 mM in NaP_i) with a peak extinction at 579 nm were normalized for a better comparison (Figure S19).

XAS sample preparation

Table S1. Samples for XAS analysis.

1	powder
3.2 µM **1**, 30 mM NaP_i	solution
3.2 µM **1**, 30 mM NaP_i, 1.5 mM $[Ru(bpy)_3](ClO_4)_3$	solution
1 mM **1**, 30 mM NaP_i	solution
1 mM **1**, 30 mM NaP_i, 8 mM $[Ru(bpy)_3](ClO_4)_3$	solution
CoCat	film

The powder of **1** was 'diluted' with Boron nitride (SIGMA ALDRICH CHEMIE GMBH MUNICH, GER) at a ratio of 1:10. A single layer of Kapton tape (0.025 mm, Goodfellow, Bad Nauheim, GER) was fixed on both sides of the mount. This mount was a custom-made, 3 mm polyoxomethylene sheet, which has a 0.5 x 1.5 cm² window through which the samples are accessible in XAS measurements. XAS samples of **2** were prepared in the same way.

A first Kapton tape (25 µm, Goodfellow, Bad Nauheim, GER) was fixed on one side of the custom-made sample-holder frame. The frame was a 3 mm thick polyoxomethylene sheet with a 0.5 x 1.5 cm² window hole through which the samples are accessible in XAS measurements. The powder samples were filled into the frame backed by the first Kapton tape. The cavity filled with the sample powder was closed by a second Kapton tape. XAS samples of **2** were prepared in the same way.

The liquid-sample mounts were manufactured as described above and closed with Kapton tapes on each side resulting in an initially empty volume between the Kapton layers of 200 µL. In variance to the powder-sample holders described above, the polyoxomethylene frame contained two holes (or channels) with a diameter of about 1 mm, to facilitate injection of a solution using a syringe.

For measurements on **1** after completion of the oxygen-evolution reaction, solutions of $[Ru(bpy)_3](ClO_4)_3$, and **1** in 30 mM NaPi were de-aerated by bubbling with argon gas for 10 minutes. Then the two solutions were quickly combined yielding the final concentrations indicated in Table S1. Within about 10 minutes after mixing, they were injected with a gas-tight Hamilton syringe (Sigma Aldrich Chemie GmbH Munich, GER) into the liquid-sample holders (described in the preceding paragraph, volume of 200 µL) through one of its holes. In separate control experiments using a Clark-type O_2-electrode, we had verified that the reaction is relatively fast and essentially completed within 50 s (> 90% of maximal amount of O_2 formation). Accordingly, the samples were promptly frozen in liquid nitrogen after a reaction time in the sample holder of 40 s yielding an overall reaction time of about 50 s (ca. 10 s before and during injection into the sample holder + 40 s after injection).

The CoCat film was prepared using a SP-200 potentiostat (Bio-Logic SAS, Claix, France). Potentiostatic electrodeposition was carried out at 1.05 V *vs.* NHE in 0.1 M KP_i, pH 7 (prepared as a mixture of 40 % KH_2PO_4 and 60 % K_2HPO_4 followed by adjustment of the pH) and 0.5 mM Co^{2+} in a three electrode set-up. Potentials were corrected for iR drop, R was equal to 50 Ω (for the entire cell). Deposition was completed, when a charge of 5 $mC \cdot cm^{-2}$ had passed. The working electrode was a thin layer of conducting indium tin oxide (ITO) on glass with dimensions 1.0 cm x 2.5 cm, the counter electrode a platinum wire, and the reference a $Hg/Hg_2SO_4/K_2SO_4$ electrode. The resulting CoCat sample was carefully rinsed with 0.1 M KP_i. Then, the sample was conditioned at 1.05 V in Co-free electrolyte for 2 min. Finally, the sample was quickly blow-dried using dry air. A single layer of Kapton tape (50 µm, Goodfellow GmbH) was used to fix the sample on its mount (custom-made, 1 mm thick polyvinyl chloride (PVC) sheet which has a 1.1 x 1.5 cm^2 window). The CoCat electrode was fixed on the mount with Kapton tape. Finally, the mounted CoCat was frozen in liquid nitrogen within 1 min after conclusion of the conditioning step. All samples were stored for no longer than two weeks before the synchrotron measurement. The Bio-XAS setup and the data extraction at the Co-K-edge are already described elsewhere.[S1]

EXAFS simulations. All simulations were performed using the in-house software package SimX lite. The EXAFS data were extracted as described elsewhere[S1] (spline range 7711-8511.65 eV, number of knots = 2, $E_o = 7710$), then weighted by k^3 and simulated (least-squares fit) in k-space (without any Fourier-filtering). The phase functions for the EXAFS spectrum were obtained by *ab-initio* calculations using Feff 9.05.[S2-3] For the simulation of all **1** containing samples, the coordinates were obtained from the XRD data of **1**. The energy shift of E_0 (relative to the value used for extraction of the experimental EXAFS data, that is, 7710 eV) was 3.5 eV.

Synthesis

Synthesis of $Na_{10}[Co_4(H_2O)_2(PW_9O_{34})_2]\cdot 27H_2O$, 1. The preparation of **1** was performed analogously to the synthesis of its potassium derivative $K_{10}[Co_4(H_2O)_2(PW_9O_{34})_2]\cdot 20H_2O$ reported by FINKE et al.[S4] setting out from B–$Na_8H[PW_9O_{34}]$, which had been dried for 2 hours at 140 °C at 1 atm. Solid B–$Na_8H[PW_9O_{34}]\cdot 19H_2O$ (2.00 g, 0.7 mmol, 1 equiv.) was dissolved in 10 mL of water. To this colorless solution solid $Co(NO_3)_2\cdot 6H_2O$ (0.41 g, 1.4 mmol, 2 equiv.) was added while stirring at ambient temperature. The resulting purple suspension was heated to 60 °C for 20 minutes and a deep purple solution resulted. To this hot reaction mixture solid NaCl (1.20 g) as well as 1 mL EtOH were added and the solution was heated to 80 °C for 1 hour. A purple to violet crystalline solid precipitated upon cooling to room temperature overnight. The solid was collected by filtration, washed three times with 1 mL of ice cold water and recrystallized from a minimum amount of hot water (70 °C) with cooling to room temperature overnight. After filtration and drying in vacuo **1** was isolated as purple violet crystals (0.957 g, 48% based on Co). The basic structure and purity of the compound was confirmed by FT-IR, single crystal XRD, EXAFS, UV/Vis spectroscopy and ESI-MS.

Synthesis of $Na_{17}[((Co(OH_2))Co_2PW_9O_{34})_2(PW_6O_{26})]$, 2. Compound **2** was synthesized according to the literature.[S5] The purity of the compound was confirmed by FT-IR, EXAFS.

Synthesis of $[Ru(bpy)_3](ClO_4)_3$. The following manipulations were carried out in a glovebox, or else by means of Schlenk-type techniques involving the use of a dry argon atmosphere. $[Ru(bpy)_3]Cl_2\cdot 6H_2O$ is commercially available from SIGMA ALDRICH CHEMIE GMBH MUNICH (GER). $[Ru(bpy)_3](ClO_4)_3$ was synthesised according a slightly modified literature procedure.[S6] An orange solution of $[Ru(bpy)_3]Cl_2\cdot 6H_2O$ (500 mg, 0.668 mmol, 1 equiv.) in 7 mL of pure water was treated with solid $NaClO_4\cdot H_2O$ (281.5 mg, 2.004 mmol, 3 equiv.) at ambient temperature and stirred for 2 minutes. The resulting intensely orange suspension was cooled to 0 °C and left without further stirring for 5 minutes. After filtering at 0 °C the residue was washed twice with 2 mL of ice cold water. Subsequently, the orange solid was dried under reduced pressure overnight, yielding $[Ru(bpy)_3](ClO_4)_2$ as an orange powder quantitatively. PbO_2 (159.8 mg, 0.668 mmol, 1 equiv.) and 20 mL of acetonitrile were added to the orange powder, and the resulting orange solution was treated with 70% $HClO_4$ (227.5 μL, 6 equiv.). A dark green to blue suspension is formed immediately and stirred for 5 minutes. The solution was filtered off from unreacted PbO_2, followed by removing of all volatiles in vacuo to yield a green residue, which was reprecipitated from 30 mL of a

MeCN/Et_2O mixture (v:v, 2:1) and washed twice with 2 mL of ice cold water. After drying under reduced pressure pure $[Ru(bpy)_3](ClO_4)_3$ was isolated as a green powder (330 mg, 0.380 mmol, 57% based on $[Ru(bpy)_3]Cl_2 \cdot 6H_2O$). Elemental analysis calc. (%) for $C_{30}H_{24}Cl_3N_6O_{12}Ru$ (867.97 $g \cdot mol^{-1}$): C 41.51, H 2.79, N 9.68; found: C 41.69, H 2.88, N 10.14.

Spectroscopic data

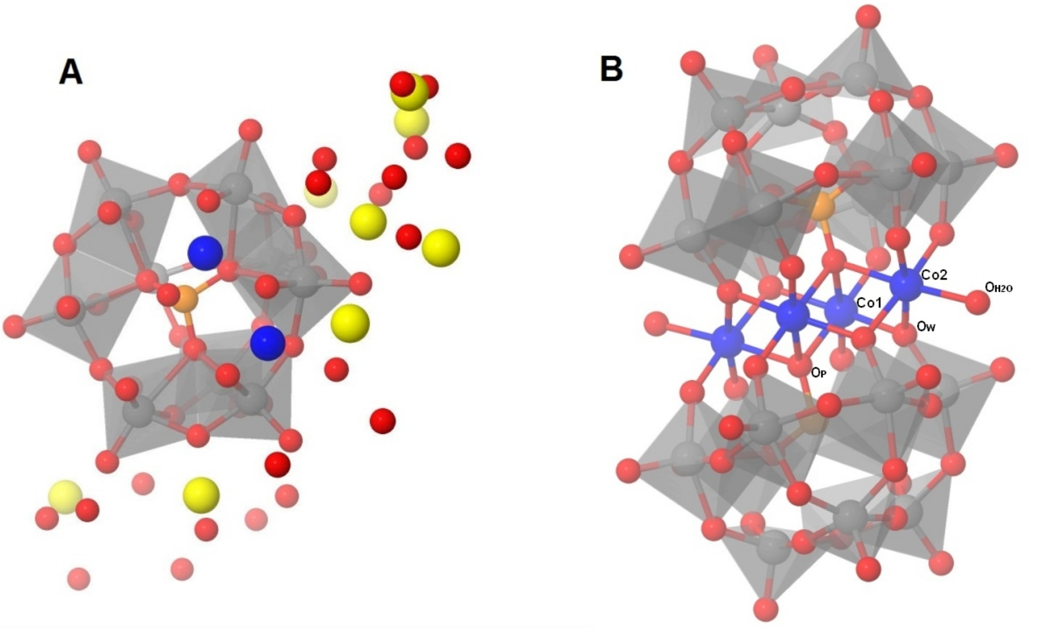

Figure S1. Coordination polyhedra representation of $[Co_4(H_2O)_2(PW_9O_{34})_2]^{10-}$ based on the single crystal X-ray diffraction data of **1**$\cdot 27H_2O$ as determined in this study. Hydrogen atoms are omitted for clarity. (A) The unit cell of **1** in plane (1 1 0). (B) The planar tetra-cobalt core with two trans coordinated water molecules sandwiched by two polyoxometalate ligands. Selected bond lengths (Å) and angles (°): Co1-Co2 3.1796(18), Co1–O_P 2.194(8), Co1-O_W range 1.998(8)-2.063(7), Co2–O_W range 2.088(8)-2.096(8), Co2–O_{H2O} 2.113(7), O_W–Co2–O_W range 82.5(3), O_W-Co2-O_{H2O} range 98.3(3)-101.1(3). Co (blue), W (grey), O (red), P (orange), Na (yellow).

Table S2. Crystal data and refinement parameters for the X-ray structure of **1**.

complex	**1**
molecular formula	$Co_4H_{20}Na_{10}O_{108}P_2W_{18}$
formula wt. (g mol^{-1})	5564.86
temperature (K)	100(2)
radiation (λ, Å)	0.71073
crystal system	triclinic
space group	*P-1*
a (Å)	11.4798(2)
b (Å)	13.2770(3)
c (Å)	18.2209(4)
α (°)	71.135(2)
β (°)	73.672(2)
γ (°)	73.251(2)
Volume ($Å^3$)	2461.78(9)
Z	1
Density (calculated)	3.754 mg/m^3
μ (mm^{-1})	21.786
F(000)	2444
crystal size (mm^3)	0.200 x 0.173 x 0.140
θ range for data collection	2,10 to 29.00 °
index ranges	$-15 \leq h \leq 15$, $-18 \leq k \leq 16$, $-24 \leq l \leq 24$
reflections collected	69901
independent reflections	13066 [R(int) = 0.1638]
absorption correction	numerical
max. and min. transmission	0.1353 and 0.0376

refinement method	full-matrix least-squares on F^2
data / restraints / parameters	13066 / 0 / 651
goodness-of-fit on F^2	0.998
final R indices [R > 2σ (I)]	$R1$ = 0.0477, $wR2$ = 0.1161
R indices (all data)	$R1$ = 0.0602, $wR2$ = 0.1211
largest diff. peak and hole	6.352 and -5.573 e.A^{-3}

Table S3. Peak identification of the ESI-MS data for **1** at near neutral pH.

Recorded m/z	**Predicted m/z**	**Peak Assignment**
932.7346	932.9119	$[Co_3(PW_9O_{34})_2NaH_6]^{5-}$
937.1325	937.3083	$[Co_3(PW_9O_{34})_2Na_2H_5]^{5-}$
939.5337	939.8991	$[Co_4(PW_9O_{34})_2H_5]^{5-}$
944.3311	944.2954	$[Co_4(PW_9O_{34})_2NaH_4]^{5-}$
948.5319	948.6918	$[Co_4(PW_9O_{34})_2Na_2H_3]^{5-}$
1175.6661	1175.1256	$[Co_4(PW_9O_{34})_2H_6]^{4-}$
1180.6637	1180.6211	$[Co_4(PW_9O_{34})_2NaH_5]^{4-}$
1186.161**0**	1186.1166	$[Co_4(PW_9O_{34})_2Na_2H_4]^{4-}$
1191.6572	1191.6121	$[Co_4(PW_9O_{34})_2Na_3H_3]^{4-}$
1197.154**0**	1197.1076	$[Co_4(PW_9O_{34})_2Na_4H_2]^{4-}$
1202.4002	1202.6031	$[Co_4(PW_9O_{34})_2Na_5H]^{4-}$
1208.4005	1208.0986	$[Co_4(PW_9O_{34})_2Na_6]^{4-}$
1574.8875	1574.4973	$[Co_4(PW_9O_{34})_2NaH_6]^{3-}$
1581.8831	1581.8246	$[Co_4(PW_9O_{34})_2Na_2H_5]^{3-}$
1589.5447	1589.1519	$[Co_4(PW_9O_{34})_2Na_3H_4]^{3-}$
1596.8722	1596.4792	$[Co_4(PW_9O_{34})_2Na_4H_3]^{3-}$
1604.1999	1603.8065	$[Co_4(PW_9O_{34})_2Na_5H_2]^{3-}$
1611.1938	1611.1338	$[Co_4(PW_9O_{34})_2Na_6H]^{3-}$
1618.1903	1618.4611	$[Co_4(PW_9O_{34})_2Na_7]^{3-}$

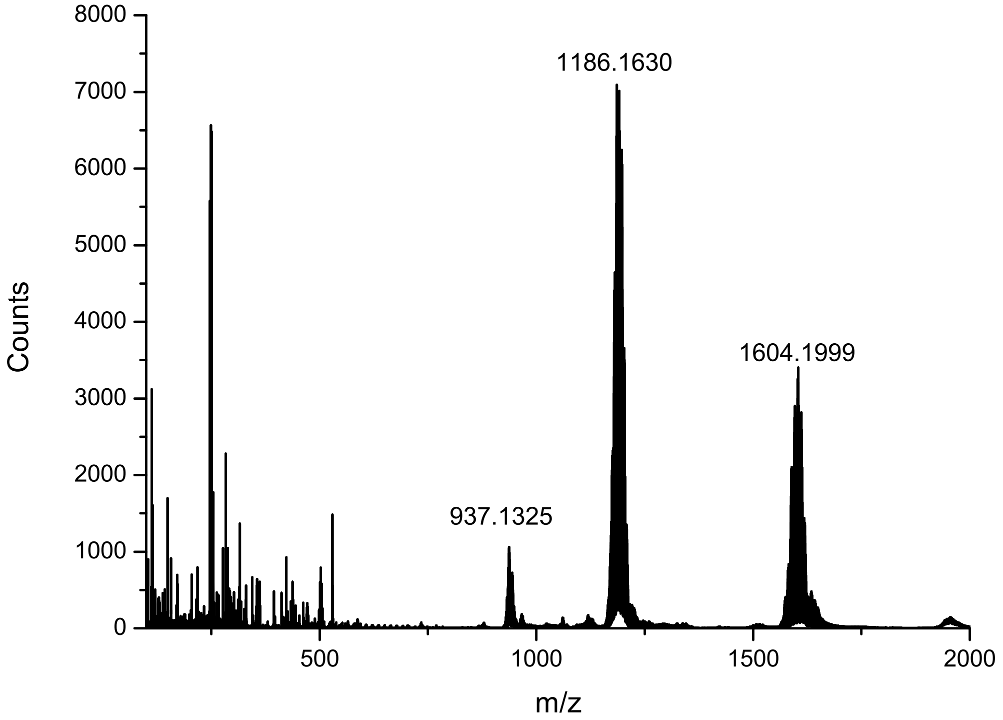

Figure S2. Full mass spectrum (ESI-MS) of **1** in H_2O:MeOH 80:20 at near-neutral pH.

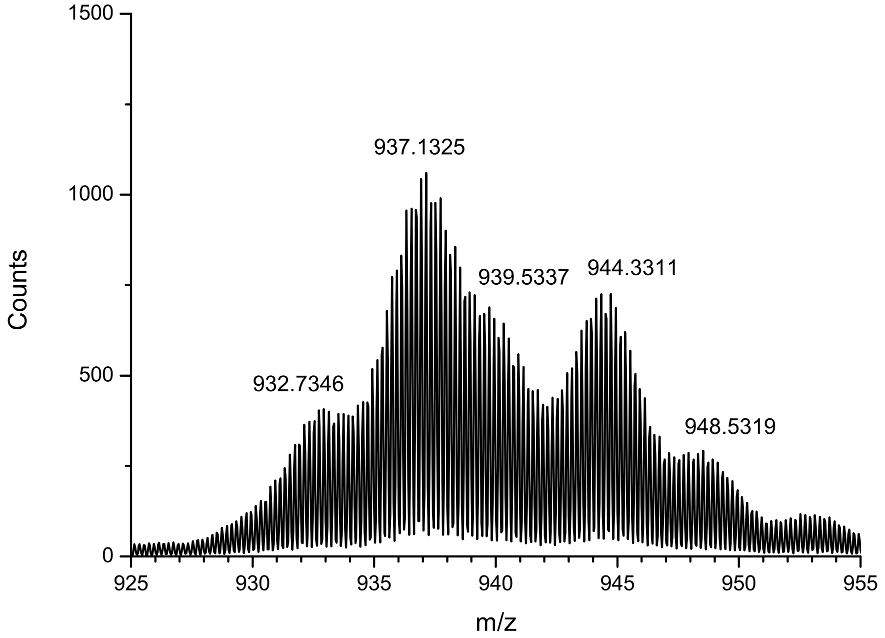

Figure S3. Measured mass spectrum of **1** from 925 to 955 m/z.

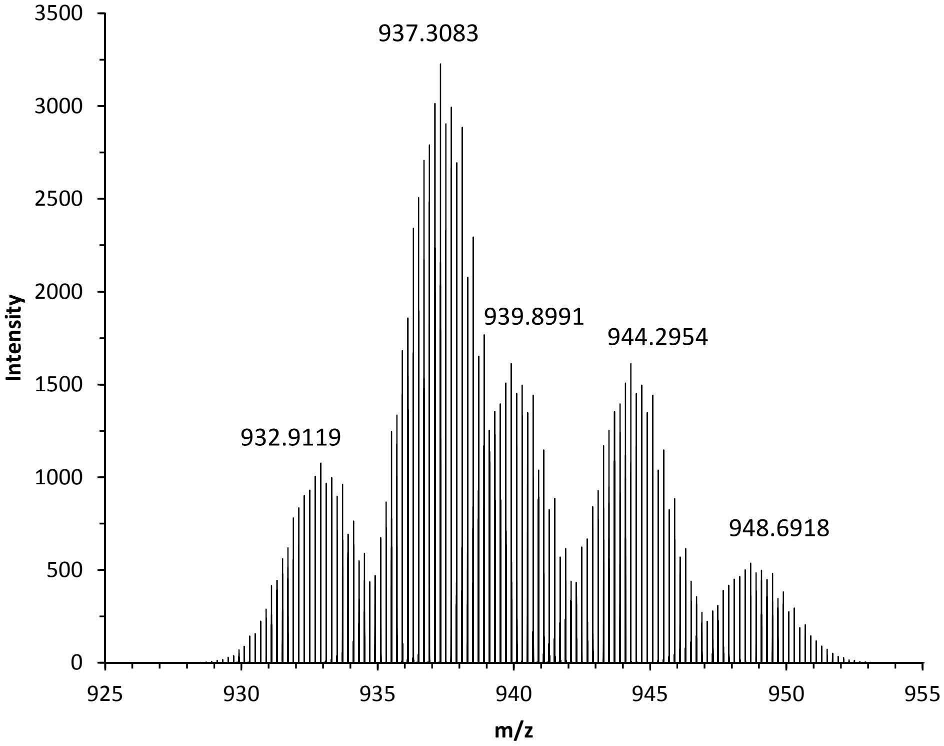

Figure S4. Simulated mass spectrum from 925 to 955 m/z.

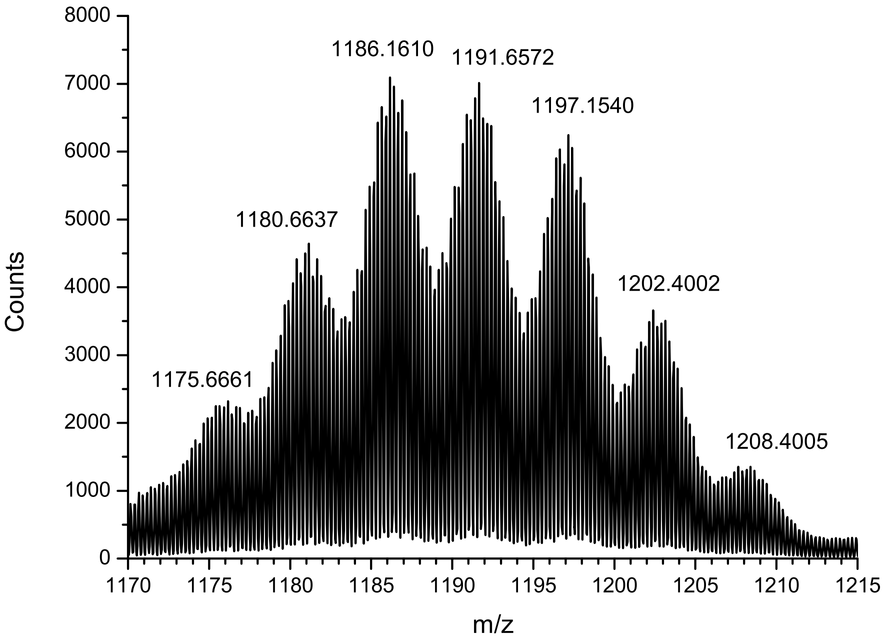

Figure S5. Measured mass spectrum of **1** from 1170 to 1215 m/z.

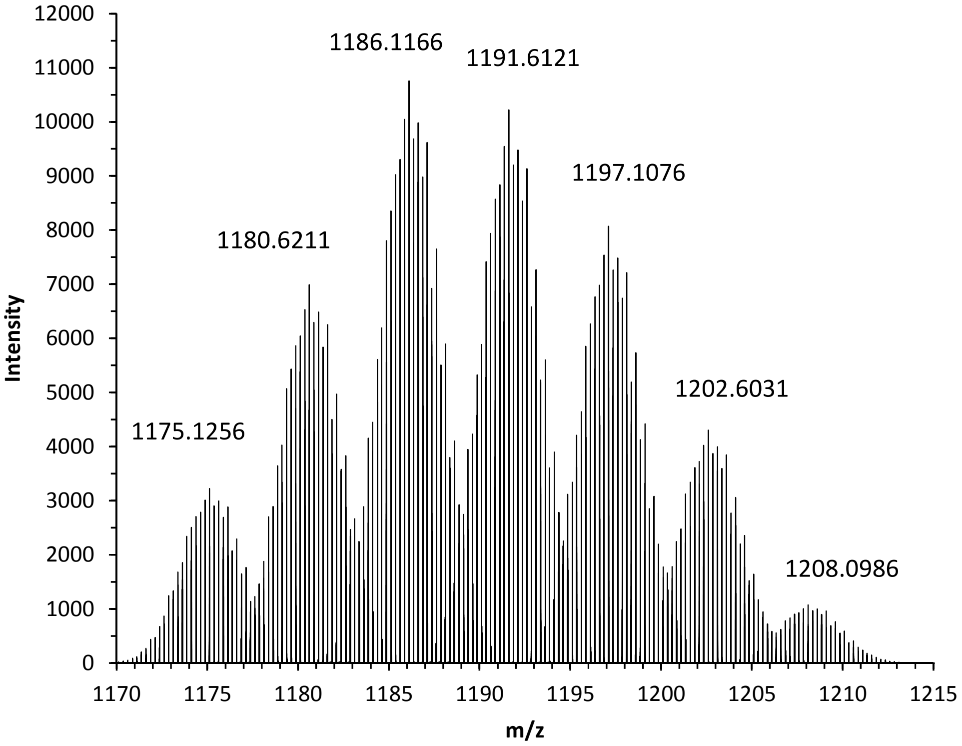

Figure S6. Simulated mass spectrum from 1170 to 1215 m/z.

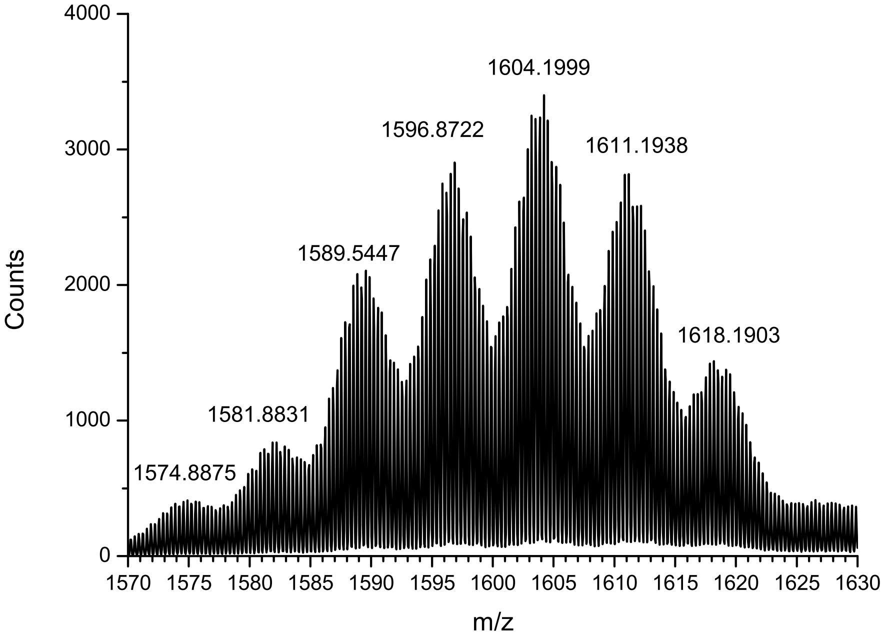

Figure S7. Measured mass spectrum of **1** from 1570 to 1630 m/z.

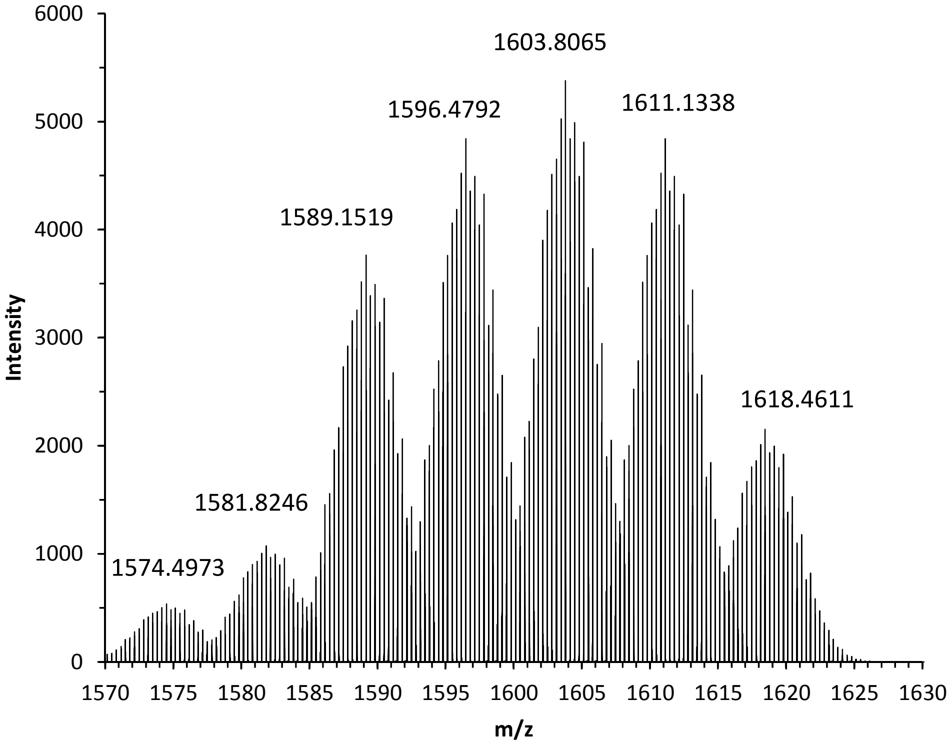

Figure S8. Simulated mass spectrum from 1570 to 1630 m/z.

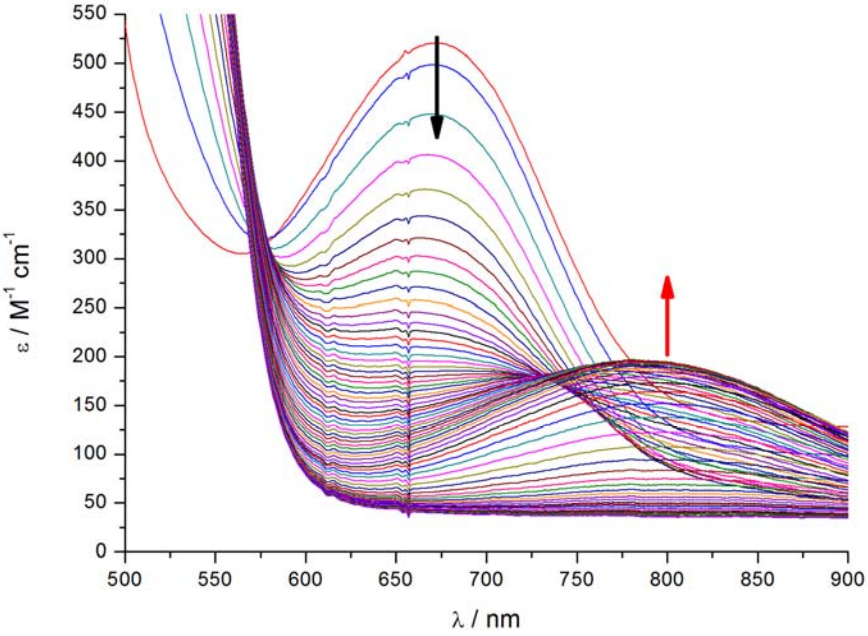

Figure S9. UV/Vis spectra of aqueous solutions of 1.5 mM in $[Ru(bpy)_3](ClO_4)_3$ in 30 mM NaP_i buffer at pH 8 from 0 to 600 seconds. Arrows indicate where the absorbance is increasing or decreasing with progress of time.

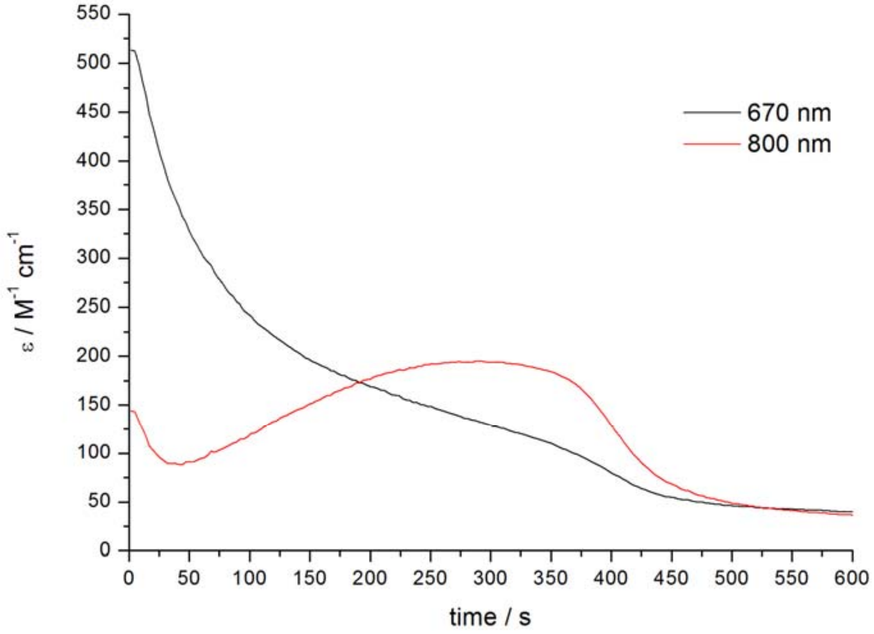

Figure S10. Monitoring of the degradation as a line diagram of ε vs. time at the designated wavelengths (670 nm black, 800 nm red) of aqueous solutions of 1.5 mM in $[Ru(bpy)_3](ClO_4)_3$ in 30 mM NaP_i buffer at pH 8.

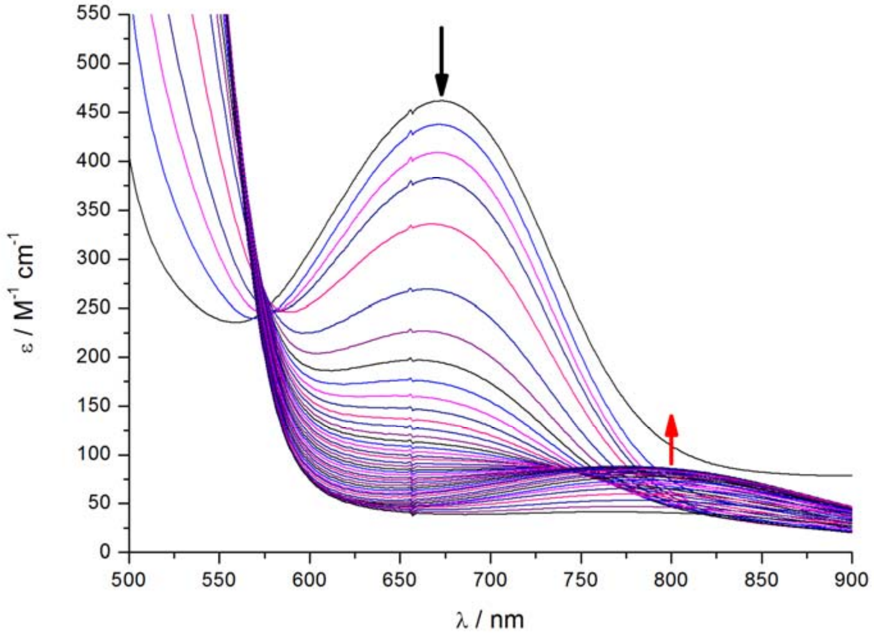

Figure S11. UV/Vis spectra of aqueous solutions of 3.2 μM in **1** and 1.5 mM in $[Ru(bpy)_3](ClO_4)_3$ in 30 mM NaP_i buffer at pH 8 from 0 to 250 seconds. Arrows indicate where the absorbance is increasing or decreasing with progress of time. Note that the band at

800 nm is less pronounced than in case of Figure S9, which can be rationalized by a repressed degradation process.

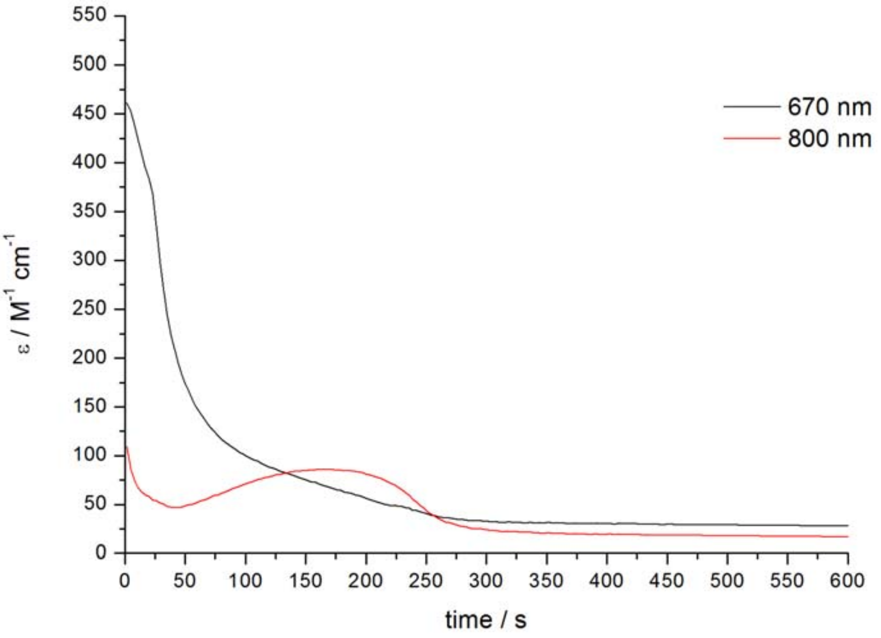

Figure S12. Monitoring of the catalytic reaction as a line diagram of ε vs. time at the designated wavelengths (670 nm black, 800 nm red) of aqueous solutions of 1.5 mM in $[Ru(bpy)_3](ClO_4)_3$ and 3.2 µM in **1** in 30 mM NaP_i buffer at pH 8. Injection was performed after 20 s.

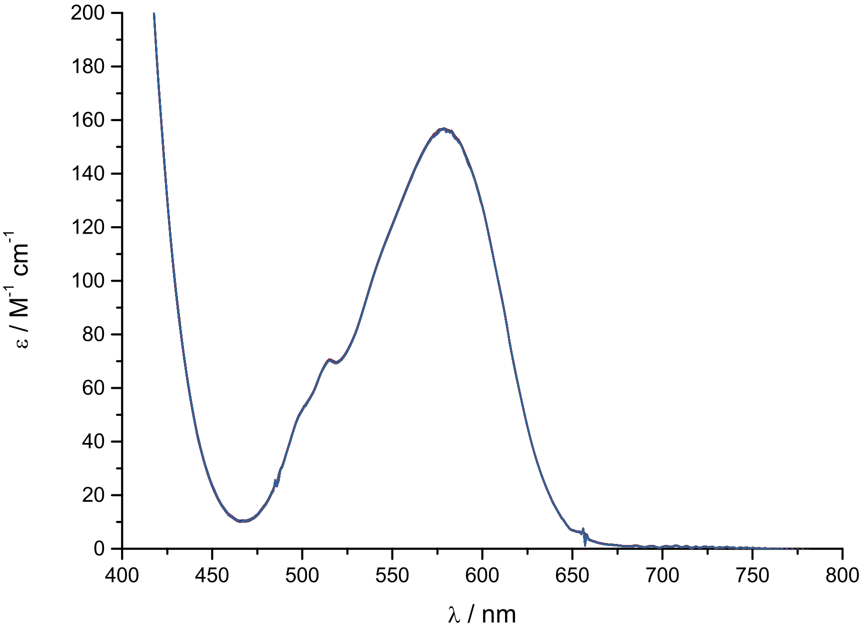

Figure S13. UV/Vis spectra of a 1 mM solution of **1** in water. For 90 minutes, spectra were taken every 10 seconds.

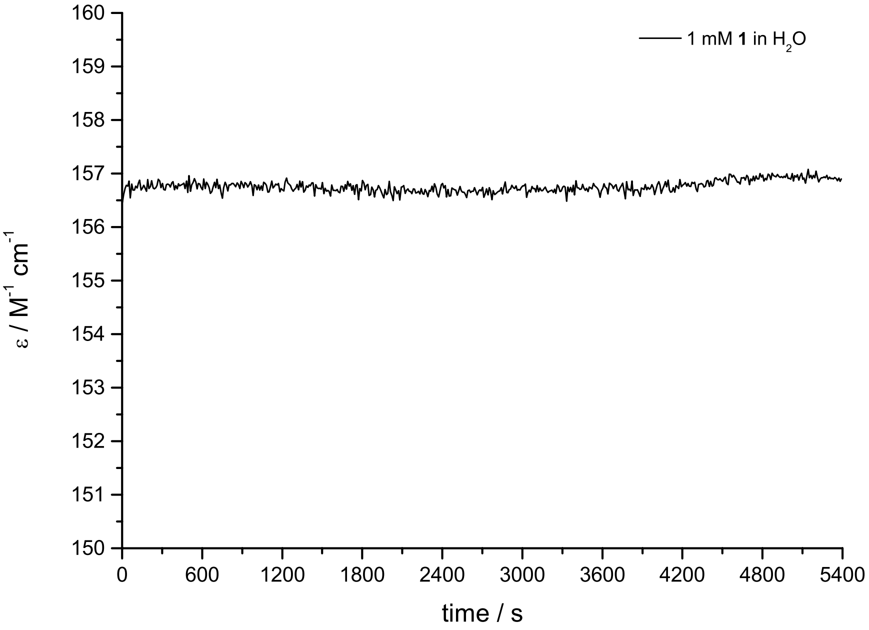

Figure S14. Peak extinction at 579 nm *vs.* time of a 1 mM solution of **1** in water. For 90 minutes, spectra were taken every 10 seconds.

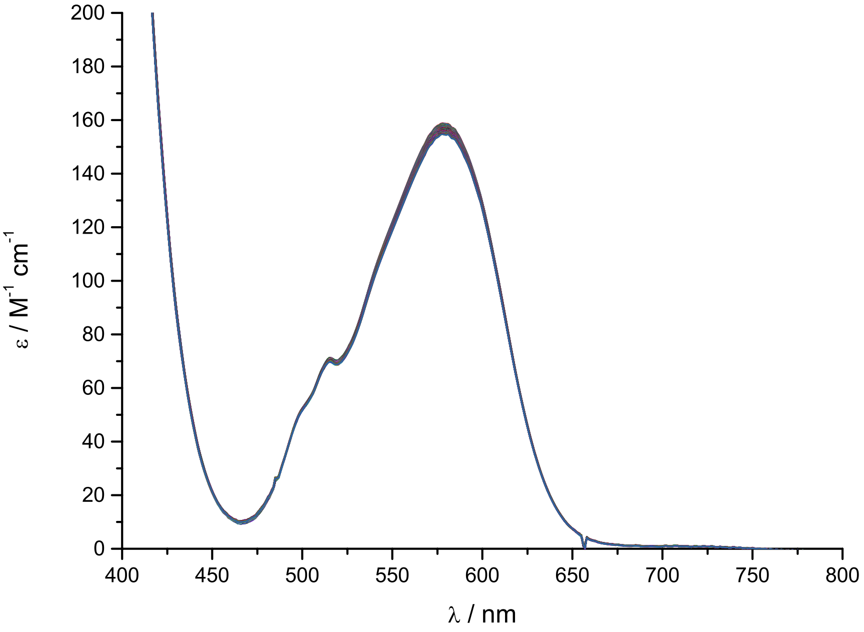

Figure S15. UV/Vis spectra of a 1 mM solution of **1** in 30 mM NaP$_i$ buffer (pH 8.0). For 90 minutes, spectra were taken every 10 seconds.

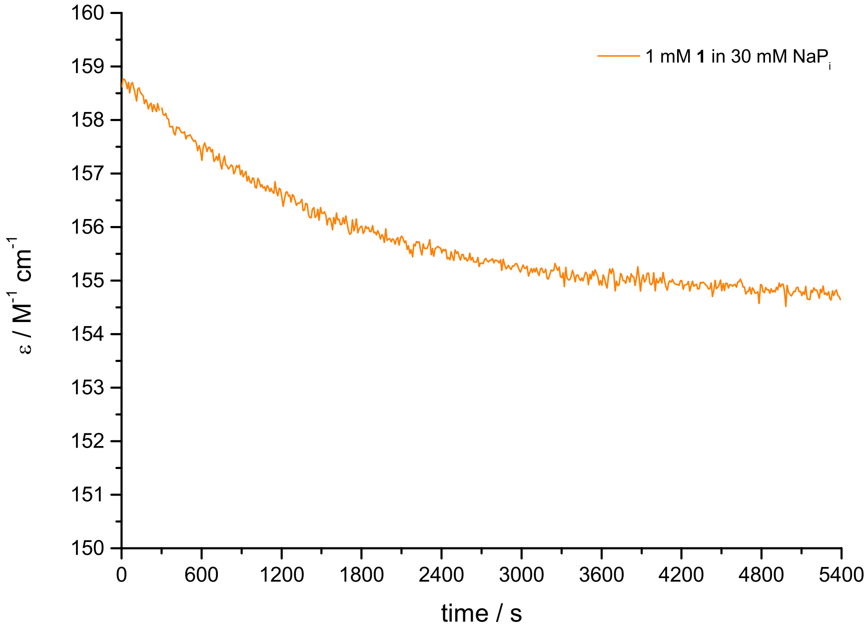

Figure S16. Peak extinction at 579 nm *vs.* time of a 1 mM solution of **1** in 30 mM NaP$_i$ buffer (pH 8.0). For 90 minutes, spectra were taken every 10 seconds.

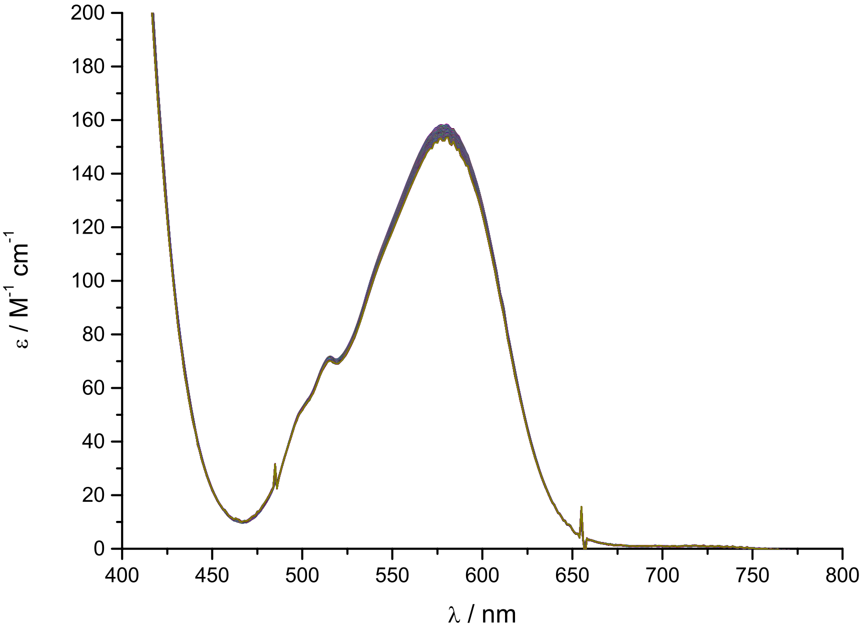

Figure S17. UV/Vis spectra of a 1 mM solution of **1** in 400 mM NaP$_i$ buffer (pH 8.0). For 90 minutes, spectra were taken every 10 seconds.

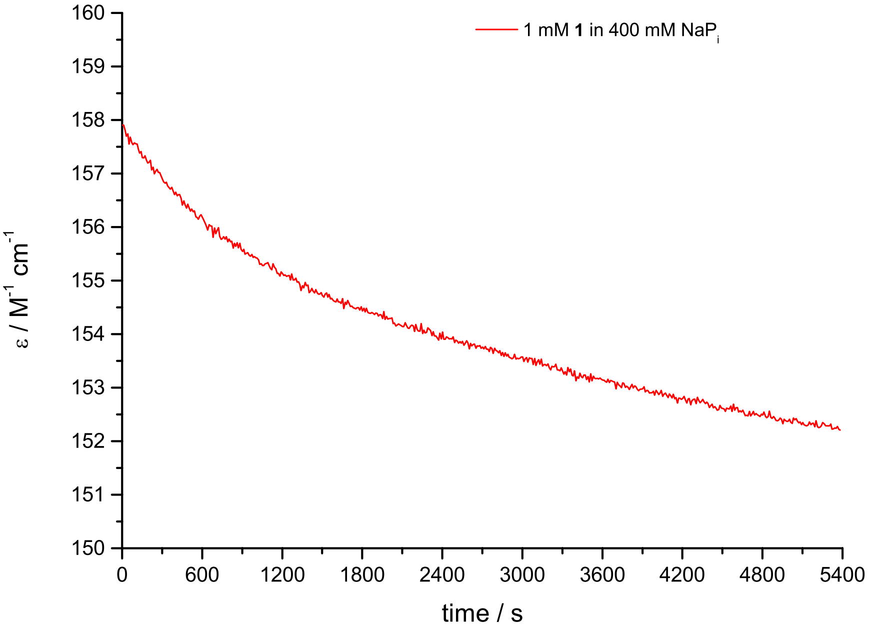

Figure S18. Peak extinction at 579 nm *vs.* time of a 1 mM solution of **1** in 400 mM NaP$_i$ buffer (pH 8.0). For 90 minutes, spectra were taken every 10 seconds.

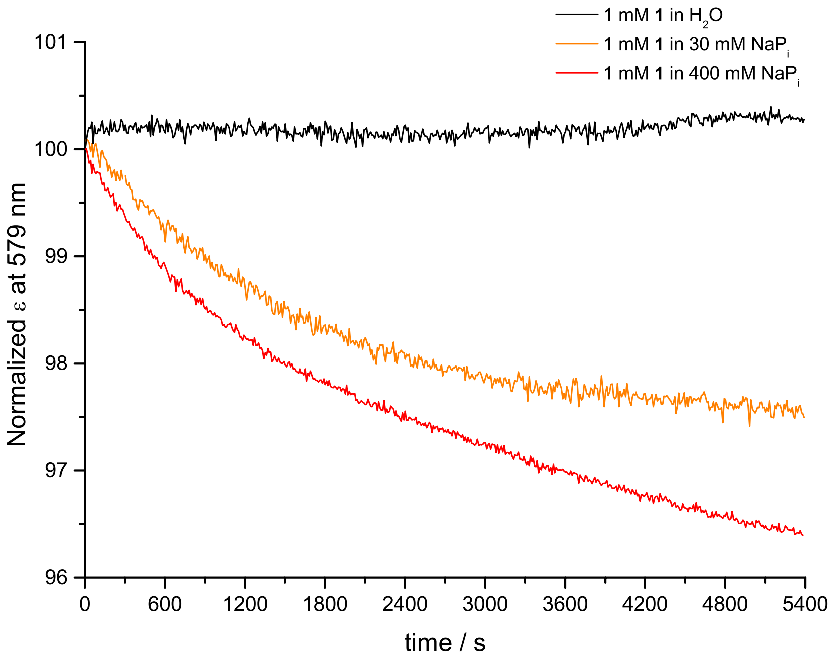

Figure S19. Normalized peak extinction at 579 nm *vs.* time of 1 mM solutions of **1** in water (black), in 30 mM NaP_i buffer (pH 8.0, orange) and in 400 mM NaP_i buffer (pH 8.0, red). For 90 minutes, spectra were taken every 10 seconds.

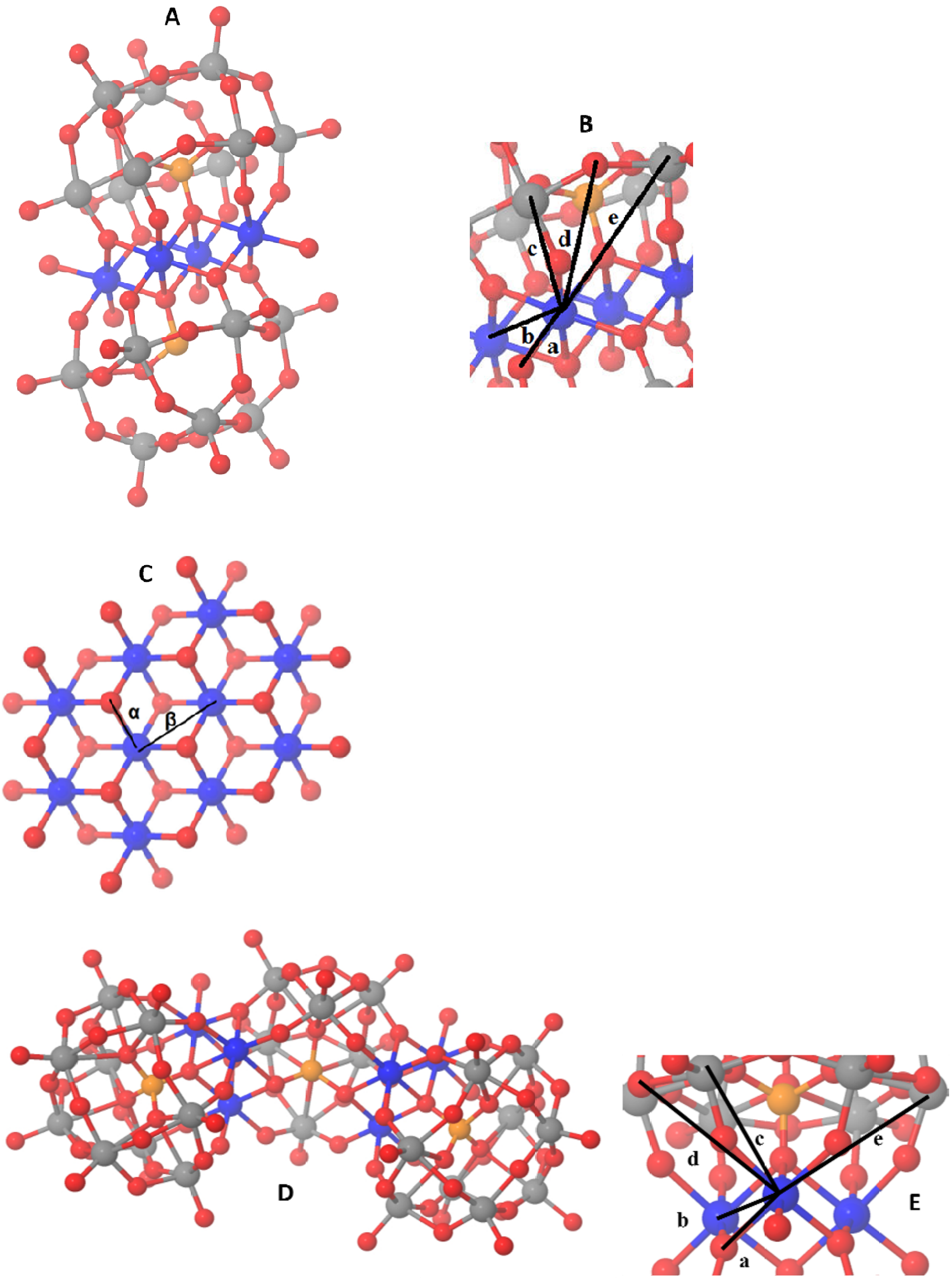

Figure S20. (A) Structure of **1**. (cobalt blue, oxygen red, phosphorous orange, sodium yellow, tungsten grey). Distances (a-e) could be identified between the absorbing Co ion and its backscattering neighbours. For detailed information see Table S2. **(B)** Enlarged picture of the quantified distances of **1**. **(C)** Structure of the CoCat with distances α and β. **(D)** Structure of **2**. **(E)** Enlarged picture of the quantified distances of **2**.

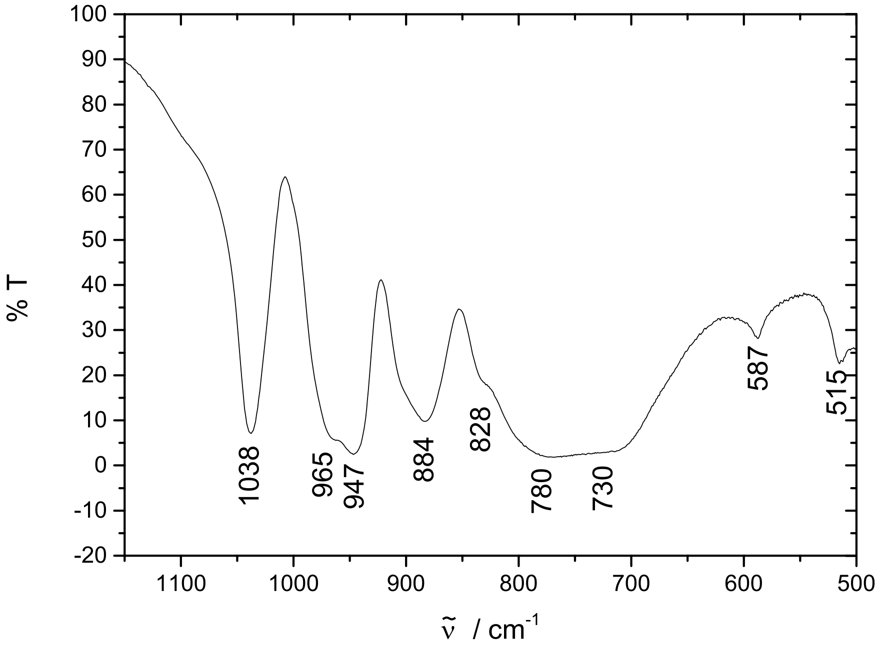

Figure S21. Infrared spectrum of $Na_{10}[Co_4(H_2O)_2(PW_9O_{34})_2]\cdot 27\ H_2O$ (**1**) (1 wt% sample in KBr pellet).

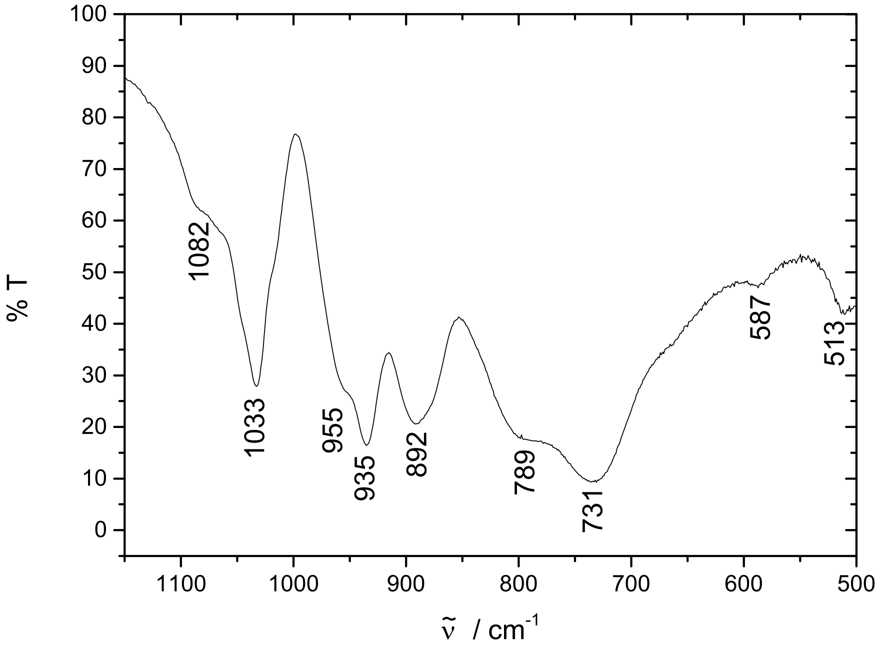

Figure S22. Infrared spectrum of $Na_{17}[((Co(H_2O))Co_2PW_9O_{34})_2(PW_6O_{26})]$ (**2**) (1 wt% sample in KBr pellet).

Table S4. Complete parameters of the EXAFS simulation presented in Table 1 of the main manuscript. All parameters were determined by curve-fitting of k^3-weighted EXAFS data (before Fourier transformation, *k*-range of 3–13 Å^{-1}). The amplitude reduction factor, S_0^2 was 0.78, and the energy axis of the fit was shifted by +3.5 eV relative to the initially selected E_0 of 7710 eV. The parameter errors correspond to the 68% confidence interval.

	Co-O(a)			**Co-Co(b)**			
Sample	N_O	R_O (Å)	σ_O (Å)	N_{Co}	R_{Co} (Å)	σ_{Co} (Å)	R_f
CoCat	6.0±0.3	1.89±0.01	0.064±0.002	4.3±0.3	2.81±0.01	0.068±0.002	17
1, Ru(bpy)$_3$	5.9±0.8	2.05±0.01	0.081*	2.4±0.4	3.19±0.01	0.044*	20
1 (l)	6.7±0.8	2.04±0.01	0.081*	2.5±0.4	3.19±0.01	0.044*	20
1 (s)	6.0±0.8	2.05±0.01	0.081*	2.5±0.4	3.19±0.01	0.044*	20

	Co-W(c)			**Co-O(d)**			
Sample	N_O	R_O (Å)	σ_O (Å)	N_{Co}	R_{Co} (Å)	σ_{Co} (Å)	R_f
1, Ru(bpy)$_3$	3.2±0.8	3.54±0.01	0.063*	6.2±1.0	4.38±0.03	0.053*	20
1 (l)	3.3±0.8	3.55±0.01	0.063*	6.6±1.0	4.38±0.03	0.053*	20
1 (s)	3.2±0.8	3.55±0.01	0.063*	6.7±1.0	4.38±0.03	0.053*	20

	Co-W(e)		
Sample	N_O	R_O (Å)	σ_O (Å)
1, Ru(bpy)$_3$	6.5±2.0	4.94±0.02	0.059*
1 (l)	4.8±2.0	4.95±0.02	0.059*
1 (s)	5.2±2.0	4.96±0.02	0.059*

Table S5. X-ray edge-position energies and estimated Co oxidation states. The integral method described elsewhere (ref. 18 of the article) was used (integration: $0.15<\mu<1.0$) for determination of edge energies; the energy at the half-height ($\mu = 0.5$) of the normalized spectra is shown for comparison. The indicated error ranges are based on standard deviations obtained by analysis of three or more XANES spectra per sample type.

Sample	Half-height (eV)	Integral (eV)	Ox. state
$Co^{III}Cat$	7720.4 ± 0.1	7720.7 ± 0.1	2.9 ± 0.1
1 (l), $[Ru(bpy)_3]^{3+}$	7718.4 ± 0.2	7718.6 ± 0.2	2.0 ± 0.2
1 (l)	7718.3 ± 0.2	7718.5 ± 0.2	2.0 ± 0.2
1 (s)	7718.3 ± 0.2	7718.5 ± 0.2	2.0 ± 0.2
2 (s)	7718.0 ± 0.2	7718.2 ± 0.2	1.8 ± 0.2
$[Co(H_2O)_6]^{2+}$	7718.3 ± 0.1	7718.4 ± 0.1	2.0 ± 0.1

References

S1. M. Risch, K. Klingan, F. Ringleb, P. Chernev, I. Zaharieva, A. Fischer and H. Dau, *ChemSusChem*, 2012, **5**, 542-549.

S2. A. L. Ankudinov, B. Ravel, J. J. Rehr and S. D. Conradson, *Phys. Rev. B: Condens. Matter*, 1998, **58**, 7565-7576.

S3. J. J. Rehr, J. J. Kas, M. P. Prange, A. P. Sorini, Y. Takimoto and F. Vila, *Comptes Rendus Physique*, 2009, **10**, 548-559.

S4. R. G. Finke, M. W. Droege and P. J. Domaille, *Inorg. Chem.*, 1987, **26**, 3886-3896.

S5. M. D. Ritorto, T. M. Anderson, W. A. Neiwert and C. L. Hill, *Inorg. Chem.*, 2004, **43**, 44-49.

S6. G. P. McDermott, P. Jones, N. W. Barnett, D. N. Donaldson and P. S. Francis, *Anal. Chem.*, 2011, **83**, 5453-5457.